

PLASMA DIAGNOSTICS IN THE OPTICAL AND X-RAY REGIONS ON THE PLASMA FOCUS DEVICE PF-4 (INSTALLATION TYULPAN)

*S.P. Eliseev, V.Ya. Nikulin, A.V. Oginov, A.A. Tikhomirov
P.N. Lebedev Physical Institute of RAS, Moscow, Russia*

The results of experiments received on the plasma focus (PF) device with energy stored equal 4 kJ are represented. Photos of the current plasma sheath (CPS), pre-pinch, sphere-like plasma formations are produced with the help of the electron-optical converter contained a gated micro-channel plate (MCP) and the CCD-camera imaging system in the visible region. The radial velocity of the CPS is about 10^7 cm/s. Neon plasma electron density measured with the help of the interferograms in the visible region and the spectrums in the soft X-ray region equals $3 \cdot 10^{18}$ cm⁻³. Electron temperature equals about 200 eV. Discharge integral photos were obtained with the help of the soft X-ray pinhole camera. Pictures with 2 μ s resolution of the plasma luminescence above PF anode region were made by CCD-camera.
PACS: 52.58.Lq, 52.59.Hq, 52.70.-m

1. INTRODUCTION

The Dense Plasma Focus is a self-focusing high current discharge in a rarefied gas. The CPS pushed by its magnetic field is pressed to the camera axis producing high-temperature dense plasma object. This plasma is a different radiations source such as soft and hard X-ray, neutron radiation, charged particles and radiation the visible region. Therefore Plasma Focus is considered not only as a source for the inertial confinement fusion (ICF) with homogeneous irradiation of the X-ray [1], but also for high density lithography [2, 3], X-ray microscopy, radiography [4] and materials modification [5].

Investigations with such gas filling as neon, argon, heavy hydrogen and their mixes are represented in this article. Modification of the research parameters at gas puff and a capacitor bank voltage changing was observed frequently.

In this paper, we intend to make the mechanism of the soft X-ray generation more clearly. For this purpose was used measurements with an imaging Bragg spectrometer, a high speed imaging system at the base of electron-optical converter with MCP in the visible region, the soft X-ray pinhole camera and a laser shadowgraphy and interferometry.

2. APPARATUS

2.1. PLASMA FOCUS FACILITY

A Mather type plasma focus facility was used to generate a current sheet for compressing filled high Z gases. The discharge occurred between two single-axis electrodes. The diameter of the inner (anode) and the outer (cathode) electrodes were 30 mm and 53 mm, respectively. Their lengths were 60 and 55 mm, respectively. The condenser bank consisted of 4x12 μ F, 25 kV capacitors. The facility operated at the bank voltage from 8 to 14 kV and the total current did not exceed 0.4 MA at its maximum. Gas pressure in different experiments was from 0.3 to 6 Torr.

Fig.1 shows the photo facility with different diagnostics, Fig.2 is a Plasma Focus with moving current sheath view.

2.2. DIAGNOSTICS

A variety of diagnostics were employed to obtain more detailed information about macroscopic behavior of the CPS and plasma emission.

Electron-optical converter with MCP was used to obtain photos of the CPS and plasma dynamics with high (3 ns) temporal resolution. A digital camera NIKON-750 recorded screen luminosity. The 200 μ m pin-hole was installed before electron-optical converter to obtain clear spatial image. Registration was produced under 90° to the vertical axis.

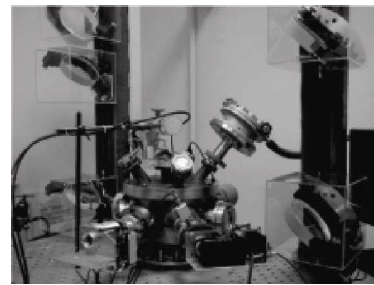


Fig.1. Photograph of the PF chamber with the different diagnostics

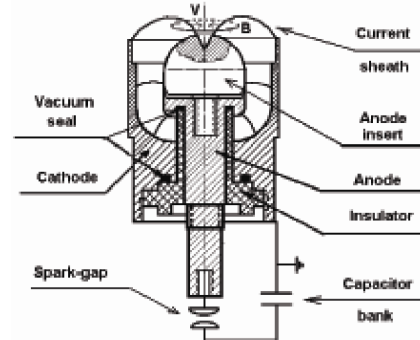


Fig.2. Plasma Focus with moving current sheath view

Registration of the region over anode plane in the visible region was carried out with the help of CCD-camera with 2 μ s resolution.

Laser shadowgraphy and interferometry were based on a single-pass Mach-Rozhdestvensky interferometer with the varying arm of 1 – 2 m, an aperture of 10 cm and Nd:YAG-laser at the second harmonics ($\lambda = 1.06$ μ m and 532 nm) with the pulse of 120 mJ for 3 ns. The plasma light was removed by an aperture placed at the focal point of the imaging lens and a glass filters mounted just before the image sensor. CCD camera with aperture of 6.5 x 4.8 mm size and 8.3 x 8.3 μ m pixel size recorded signal. The dynamics and structure of the focused plasma can be obtained with framing shadowgraphy, providing appropriate time delay between the laser probing and plasma pinching instants.

An imaging Bragg spectrometer with convex mica crystal was employed to analyze the soft X-ray emitted from the pinched plasma. A mica ($2d = 19.884$ \AA) convex crystal with the diameter of 40 mm was employed in this spectrometer. For the imaging, an entrance slit of 2.5 mm in width and 19 mm in length was used. The spectrometer was capable of collecting X-ray spectra in a 3 ... 18 \AA region with the resolving power of $R = \lambda/\delta\lambda > 500$ and the

dispersion from 0.15 to 0.05 Å/mm. The angle between the spectrum viewing direction and the plate axis was about 45°. Closeness of the measured lines permitted to avoid a spectral calibration of the spectrograph. For removing background light and to additional crystal defense from direct plasma flow 5 μm Al foil filter was arranged between an entrance slit and crystal. A RAR2494 film was employed as a recording medium.

Discharge integral photos were obtained with the help of the soft X-ray pinhole camera on the X-ray film of RAR2494 type. The diameter of the pinhole was 230 μm. Beryllium foil filter (12 μm of thickness with a pass band $\lambda < 20 \text{ \AA}$) prevented from the visible light also emitted from the source. Combination of the applied film and the Be foil filter gave a registration region from 0.3 to 20 Å.

3. RESULTS AND DISCUSSION

3.1. DYNAMICS OF THE PLASMA LUMINOSITY IN THE VISIBLE REGION

By means of the electron-optical converter with built-in MCP, photos of the plasma and current luminescence in a visible range have been taken (Fig.3). Synchronization of the moment MCP start was carried out by means of a signal from the magnetic. The time synchronization was carried out in a relation to the moment of the maximal current sheath compression, which coincide with the feature moment on a current derivative. The time exposition was about 3 ns.

In the photos obtained using neon as a filling gas, it is visible, that at the time interval of -100 ns to -200 ns before the maximal compression of the CPS when in a photo it is yet visible, on an axis of the chamber already is available obviously expressed pre-pinch. At the moments of time from -10 up to +20 ns shining areas of the spherical form have been found out. The luminescence of an evaporating metal from the anode was seen through some microseconds after the maximal CPS compression.

In the photos made by means of CCD camera with two microseconds resolution (Fig.4) the vertical current column is visible. In a different time moment the current shining zone has various widths from 2 mm up to 2...3 cm. In some photos similarity of twisting light layers is visible. It can be explained by a twisting of current. In these experiments argon was used as a filling gas.

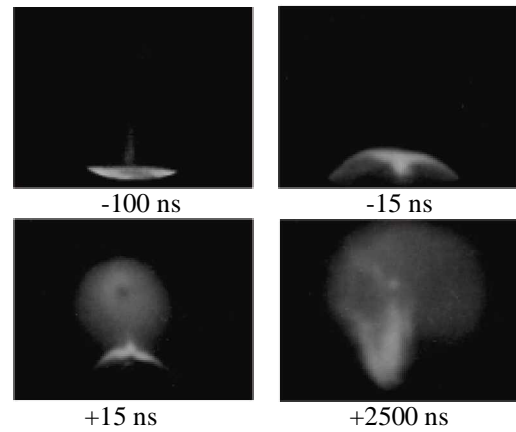


Fig.3. EOC images of the discharge in the visible light at the different instants

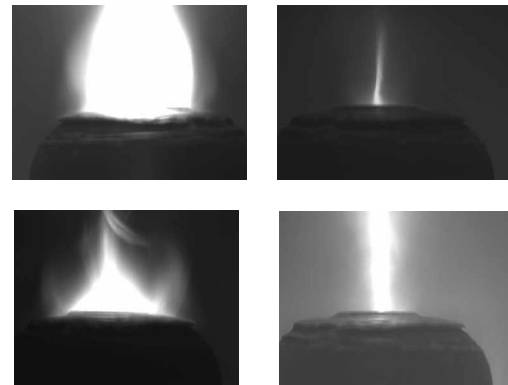


Fig.4. Images obtain by CCD camera with 2 μs exposure

3.2. INTERFEROMETRY MEASUREMENTS

On Fig.5,d the shadow photo of compressed CPS which made with use of the Nd:YAG-laser is represented. Synchronization was carried out by the photo diode impulse what arose during the moment of current sheath passage under it.

The plasma sheath during the compression phase on the PF device generally has a good quasi-cylindrical axial symmetry, hence only one perpendicular direction of laser probing may be applied, and then the Abel integral equation provides a good approximation. The obtained image is shown in Fig.5,c). The interferential fringes are singled out and the

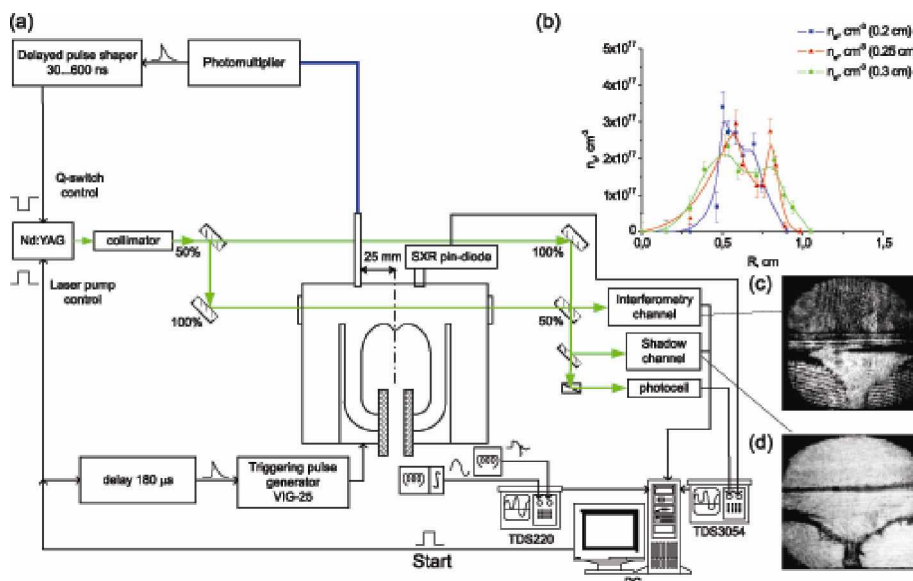


Fig.5. (a) Principal scheme of laser diagnostics and apparatus synchronization; (b) Profiles of electron density obtained at different distances from anode surface. Samples of interferometric; (c) and shadow (d) images obtained

phase distribution is determined by the fringe shifts. The calculation of the electron density profile is carried out using numerical procedure of Abel inversion. The piecewise-parabolic approximation of a refractive index profile with variable piece lengths is employed to reduce paraxial error growth. The error in the calculation was less than 10...20 percent. An example of data obtained is shown in Fig.5,b).

3.3. INTEGRAL PHOTOS AND SPECTRA IN THE SOFT X-RAY REGION

Integral plasma shining in the soft X-ray region is shown in Fig. 6. The photo has been made with the help of integral pinhole camera. The height and width of the brightest pinched plasma region were 4 and 1.5 mm, respectively. Recorded radiation lies in a band from 0.3 up to 20 Å.

Spectrum and densitogram of neon plasma, which consist of the resonance lines of the H-like and He-like ions and their satellites in region 9...14 Å is shown on Fig. 6. The spectral lines NeX 12.134 (H-like Lyman α), NeIX 13.447 (He-like resonant line), NeIX 13.549 (He-like intercombinatory line), "Member of Principal Series" (MPS) lines and a continuous radiation were registered. Initial identification of the spectra was produced using the H-like and He-like resonance lines.

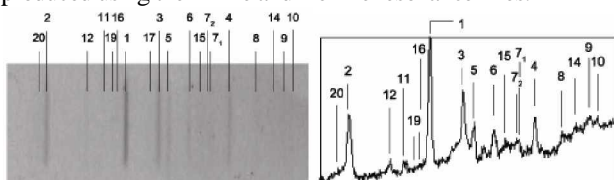


Fig.6. Spectrum and densitogram of neon plasma, which consists the resonance lines of the H-like and He-like ions and their satellites

Consequent identification was carried out by means of the following work [6]. The electron temperature was determined using the ratio of the intensities H-like (line 1 on Fig.6) and its satellite 19 ($T_e \sim 220$ eV). The electron density was calculated from the ratio of the intensities He-like resonance line 2 and intercombinatory line 20 ($N_e \sim 3 \cdot 10^{18} \text{ cm}^{-3}$) [7, 8].

Similar experiments were carried out with argon and its mixes with heavy hydrogen as a filling gas. In spite of greater features on the current derivative and significant output of neutrons for the discharge in a mix ($2 \cdot 10^8$ neutrons in 4π sr), in the given experiments spectra were not observed. The most probable explanation of this fact is that the temperature of the compressed plasma is not high enough to excite H- and He-like ions series of argon.

ДИАГНОСТИКА ПЛАЗМЫ В ВИДИМОМ И РЕНТГЕНОВСКОМ ДИАПАЗОНАХ НА УСТАНОВКЕ ПЛАЗМЕННЫЙ ФОКУС ПФ-4 (УСТАНОВКА ТЮЛЬПАН)

С.П. Елисеев, В.Я. Никулин, А.В. Огинов, А.А. Тихомиров

Приведены результаты экспериментов, проведенных на плазменном фокусе с энергетикой около 4 кДж. С помощью электрооптического преобразователя с разрешением около 3 нс получены снимки токовой плазменной оболочки, предпинча, шарообразных сгустков в видимом диапазоне. Радиальная скорость токовой оболочки $\sim 10^7$ см/с. Электронная плотность неоновой плазмы, измеренная с помощью интерферограмм в видимом диапазоне и спектров в мягком рентгеновском диапазоне, равна $3 \cdot 10^{18} \text{ см}^{-3}$. Электронная температура плазмы около 200 эВ. С помощью камеры-обскуры сделаны интегральные снимки излучения в мягком рентгеновском диапазоне. С помощью ПЗС камеры получены фотографии свечения плазмы в прианодной зоне плазменного фокуса с разрешением 2 мкс.

ДІАГНОСТИКА ПЛАЗМИ У ВИДИМОМУ І РЕНТГЕНІВСЬКОМУ ДІАПАЗОНАХ НА УСТАНОВЦІ ПЛАЗМОВИЙ ФОКУС ПФ-4 (УСТАНОВКА ТЮЛЬПАН)

С.П. Єлисеєв, В.Я. Нікулін, А.В. Огінов, А.А. Тихомиров

Приведено результати експериментів, проведених на плазмовому фокусі з енергетикою близькою до 4 кДж. За допомогою електрооптичного перетворювача з розділенням близько 3 нс отримані знімки токової плазмової оболонки, передпінча, кулеподібних згустків у видимому діапазоні. Радіальна швидкість токової оболонки $\sim 10^7$ см/с. Електронна густина неонові плазми, вимірювана за допомогою інтерферограм у видимому діапазоні і спектрів у м'якому рентгеновському діапазоні, дорівнює $3 \cdot 10^{18} \text{ см}^{-3}$. Електронна температура плазми близько 200 еВ. За допомогою камери-обскури зроблені інтегральні знімки випромінювання в м'якому рентгеновському діапазоні. За допомогою ПЗС камери отримані фотографії світіння плазми в прианодній зоні плазмового фокуса з розділом 2 мкс.

The particular advantage of used methods is simultaneous measuring of the electron temperature and density by means of the groups of the nearby lines the same elements that allowed to attribute obtained values N_e and T_e to the same area. Besides, using gases with different charges of the nucleus will permit to measure higher electron densities up to $N_e \sim 10^{23} \text{ cm}^{-3}$.

CONCLUSIONS

The dynamic behavior of the PF discharge in the visible region was observed using shadow method on the base of the Mach-Rozhdvestvensky interferometer, photographing with the help of the electron-optical converter and CCD-camera imaging system. The existence of pre-pinch in the time range from -10 up to +20 ns relative to peculiarity on the current derivative was demonstrated sphere-like shining.

Using the convex Bragg spectrometer, we obtained the monochromatic images of the soft X-ray spectral lines for the NeX Lyman series and for the NeIX series. In similar experiments with argon and its mixes with heavy hydrogen similar series is not revealed. Most probably, it is caused by insufficient plasma temperature.

The electron temperature and density of the plasma hot spots were estimated by several methods. Electronic temperature ~ 200 eV has been received from relative intensities of the resonant lines and their satellites. Using relative intensity of intercombinatory and resonance lines NeIX the electronic density of plasma $\sim 3 \cdot 10^{18} \text{ cm}^{-3}$ has been calculated. The same result within experimental accuracy has been received by means of interferometry measurements.

REFERENCES

1. R.J. Leeper et al. // *Extended synopses 17th IAEA Fusion Energy Conference*, International Atomic Energy Agency, IAEA-CN-69, 1998, p. 15.
2. J.S. Pearlman, J.C. Riordan // *J. Vac. Sci. Technol.* 1981, v. 19, p. 1190.
3. I. Fomenkov. Performance of a dense plasma focus light source for EUV lithography // *2nd Int. EUVL Symp.* 2003.
4. S. Hussian, M. Shafiq, R. Ahmad, A. Waheed, M. Zakauallah // *Plasma Sources, Sci. Technol.* 2005, v. 14, p. 61-69.
5. L.I. Ivanov, A.E. Dedyurin, I.V. Borovitskaya, O.N. Krokhin, V.Ya. Nikulin, S.N. Polukhin, A.A. Tikhomirov, A.S. Fedotov // *Pramana-J.Physics.* Dec.2003, v. 61, №6, p. 1179.
6. R.L. Kelly // *J. Phys. Chem. Ref. Data*, 1987, v.16, № 1.
7. L.P. Presnyakov // *Uspekhi Fizicheskikh Nauk.* May, 1976, v.119, №1, p. 49-73 (in Russian).
8. L.A. Vainstain. Dielectronic recombination // *Trudy FIAN*, v.119, p. 1-12 (in Russian).